Survey of PMT Photocathode Quantum Efficiencies

Steve Mitchell

University of Colorado at Boulder
ECEN 5645 Spring 2008

1.0 Introduction

Photomultiplier tube (PMT) history begins in the early 1900s with Austin and Starke. The duo were the first to report on secondary emissive surfaces when they noticed that metal surfaces impacted by cathode rays emitted a larger number of electrons than were incident. Using secondary emission for the purposes of signal amplification was reported as early as 1919. Iams and Salzberg of RCA reported on a single-stage photomultiplier used for movie sound pickup in 1935. The device consisted of a triode photomultiplier tube with a photocathode combined with a single-stage dynode, producing a gain near eight [1,2].

By 1936, Zworykin and his team at RCA developed a photomultiplier tube consisting of multiple dynode stages. The tube utilized both electric and magnetic fields to direct electrons from stage to stage. This resulted in high gain, but also led to various difficulties. Namely, adjustment of the magnetic field was critical. Changing the gain by reducing the applied voltage required the magnetic field to be adjusted as well. Additionally, the open structure of the tube often led to high dark current due to feedback from ions as well as light development near the output of the device [1,2].

The first commercially successful photomultiplier tube was the type 931, first described by Zworykin in 1939 and later by Rajchmann and Janes. The PMT consisted of a compact circular array of nine dynodes utilizing electrostatic focusing. The photocathode consisted of Ag-O-Cs but was later replaced with Sb-Cs. The 931 set the industry standard in photomultiplier tube technology. In the years that have followed, various materials have been used as photocathodes, a survey of which is presented in this document [1,2].

2.0 PMT Fundamentals

The photomultiplier tube is a vacuum tube consisting of an input window, photocathode, electron multiplier, and an anode. The detection process begins when light passes through the input window and incidents the photocathode. Electrons in the photocathode are excited and emitted as photoelectrons into the tube vacuum. These photoelectrons are accelerated and focused onto the first dynode, resulting in multiplication by secondary electron emission. This process is repeated until the multiplied secondary electrons emitted from the final dynode are collected by the anode, which outputs the electron current to an external circuit [1].

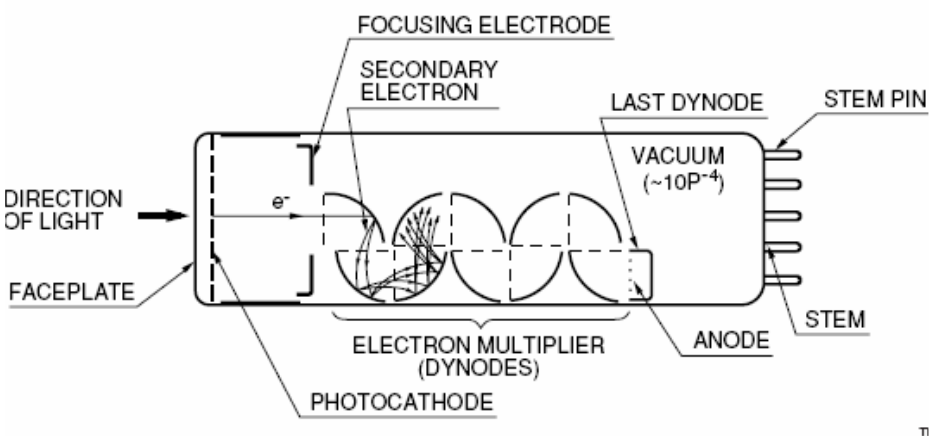

Figure 1: Fundamental PMT layout [3]

3.0 Photoelectron Emission by the Photocathode

The conversion of light entering the PMT is governed by internal photoelectric effects in which photoelectrons are excited into the conduction band. Illustrated in Figure 2, incoming photons initially strike the photocathode. The electrons in the valence band absorb the photon's energy (hv) and become excited. These excited electrons diffuse toward the photocathode surface. If the diffused electrons possess enough energy, they overcome the barrier between the valence and conduction bands in the photocathode material and are emitted into the vacuum as photoelectrons [1].

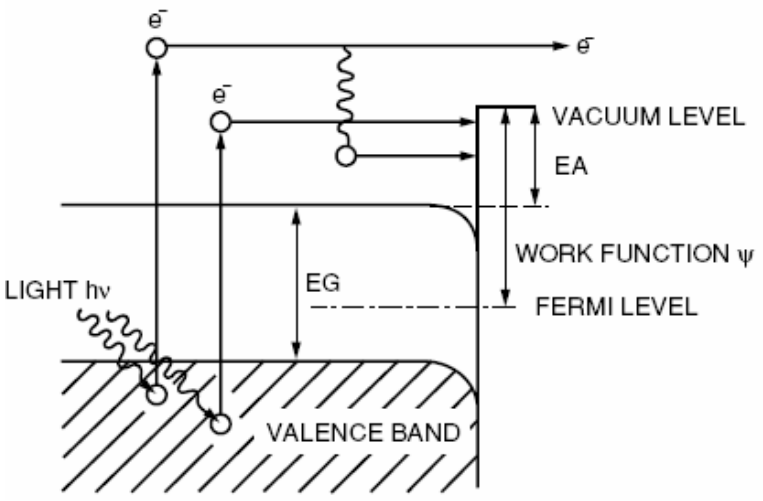

Figure 2: Photoelectric effect of a PMT photocathode [4]

The photoemission process is often expressed a probability function. Here, the quantum efficiency $\eta(\nu)$ is equal to the ratio of output electrons to incident photons.

$$\eta(\nu) = \frac{e_{output}}{h\nu_{incident}} = (1-R)\left(\frac{P_\nu}{k}\right)\left(\frac{1}{1+\frac{1}{kL}}\right)P_s \qquad (1)$$

where

R = reflection coefficient

k = full absorption coefficient of photons

P_ν = probability of photocathode electrons reaching conduction band

L = mean escape length of excited electrons

P_s = probability that electrons reaching photocathode surface will be emitted into vacuum

ν = frequency of light

From (1), it is evident that if materials have been chosen for photocathodes which determine R, k, and P_ν, the factors dominating the quantum efficiency will be L and P_s [1]. From

here, a variety of photocathode materials can be engineered with the goal of increasing the PMT's quantum efficiency.

4.0 Photocathode Materials

The majority of photomultiplier research during the later part of the 1900s has revolved around their physical configuration and the related electron optics. However, an equally important part of photomultiplier development relates to photocathode materials in an effort to increase detection efficiency. This section details the most efficient photocathodes for the infrared, visible, and ultraviolet regions.

4.1 Infrared: Ag-O-Cs (S-1)

One of the first photocathodes available for practical applications was the Ag-O-Cs, or S-1, photocathode. The structure of the photocathode consists of silver particles distributed throughout a matrix of Cs_2O with a thin layer of $Cs_{11}O_3$ on its surface. The $Cs_{11}O_3$ lowers the electron affinity at the surface so that the Ag-O-Cs is a negative electron affinity surface with a work function of 1.55 eV [5].

In this configuration, quantum efficiency levels for the Ag-O-Cs peak in the infrared around 1%, as shown in Figure 3. This peak is due to resonance absorption in the silver particles. Additionally, the low quantum efficiency in the visible is due to reflection from the film of silver on the outer surface of the photocathode [5]. While 1% quantum efficiency is low, it will be shown in Figure 4 that Ag-O-Cs has historically been the top performing photocathode for the infrared region.

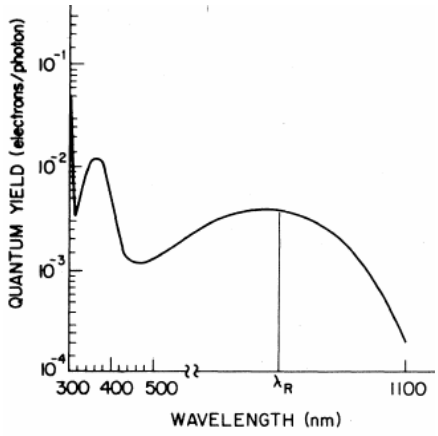

Figure 3: Quantum efficiency of the Ag-O-Cs photocathode

4.2 Visible: Na_2KSb:Cs (S-20)

During the 1950s and 60s, Sommer of RCA explored the properties of various photocathode materials, primarily alkali-antimonides. Sommer's most noteworthy contribution was the Na_2KSb:Cs, or S-20, photocathode. The Na_2KSb:Cs photocathode has a high sensitivity in the UV and visible that extends into the infrared, more than the earlier Cs_3Sb photocathode. The spectral response of Cs_3Sb was limited, barely extending through the visible. The Na_2KSb:Cs photocathode is also more stable at higher temperatures than Cs_3Sb and has a low dark emission rate. The success of Na_2KSb:Cs led the RCA team to use the photocathode as a match to the NaI:TI crystals used in scintillation counting [2].

Figure 4 illustrates the quantum efficiency of several commercial photocathodes. From the figure and [6] it is clear that the Na_2KSb:Cs photocathode (IV) has a high quantum efficiency over the visible spectrum, peaking in the UV near 30%. The photocathode has an efficiency around 10% in the red, dropping down below 1% in the infrared.

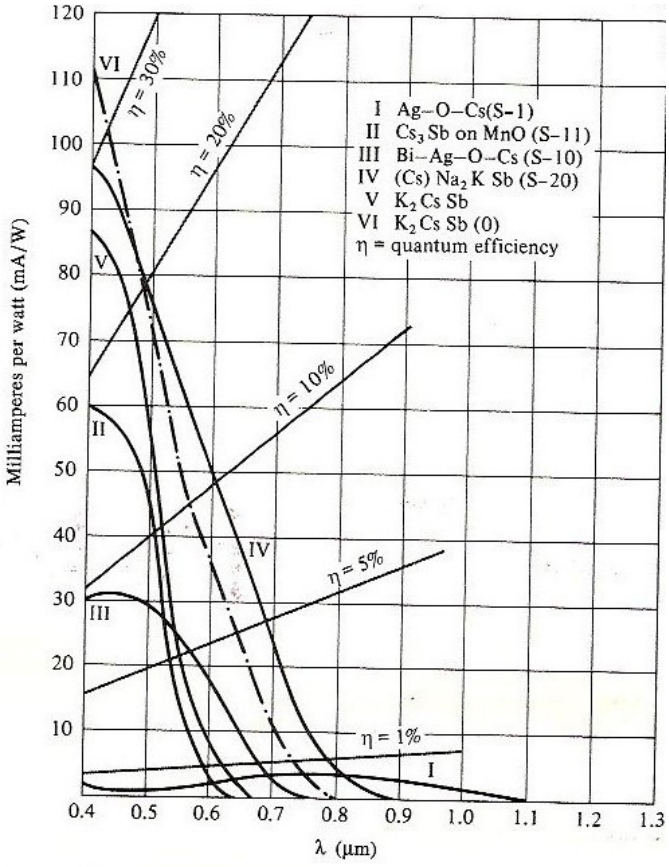

Figure 4: Quantum efficiency of the Na_2KSb:Cs (VI) photocathode [7]

4.3 Ultraviolet: K_2CsSb

Sommer [8] reports on his accidental development of the K_2CsSb photocathode in 1963. During the formulation of Na_2KSb:Cs, Sommer accidentally added the cesium before the sodium and observed an unusually high blue response before adding sodium. This accident resulted in the development of the K_2CsSb photocathode, which as shown in Figure 4, has a high quantum efficiency in the UV region. While most often used commercially for detection of blue light, K_2CsSb (VI) has quantum efficiencies approaching 30% in the UV. As a result, K_2CsSb is almost universally used commercially as a blue through UV detection photocathode [9].

5.0 Conclusions and Future Work

The majority of photocathodes used commercially were developed during the 1950s and 60s, many by Sommer and his associates at RCA. Time has proven the success of Ag-O-Cs, Na_2KSb:Cs, and K_2CsSb in detection of infrared, visible, and UV light, respectively. However, research is ongoing with the aim of increasing photocathode quantum efficiencies in each region. This section details two examples of current and future work in the detection of infrared light with increased photocathode quantum efficiencies.

5.1 $In_{.36}GA_{.31}As_{.67}P_{.33}$

La Rue et al. [10] report on the use of $In_{.36}GA_{.31}As_{.67}P_{.33}$ as an effective photocathode for detection of infrared wavelengths with efficiencies greater than Ag-O-Cs. The photocathode measures 1 mm in diameter and has a bandgap of 0.93 eV, as shown in Figure 5. The work function at the photocathode surface is reduced by an activation process consisting of a high-temperature desorption of surface oxides followed by deposition of Cs and O monolayers.

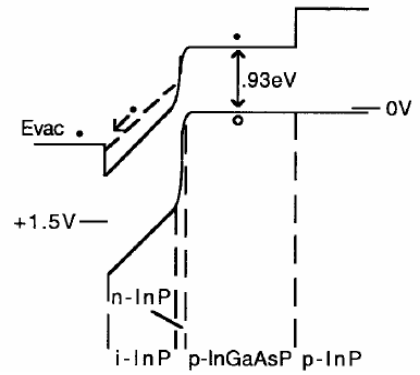

Figure 5: Band diagram of the $In_{.36}GA_{.31}As_{.67}P_{.33}$ photocathode

Quantum efficiency of the of $In_{.36}GA_{.31}As_{.67}P_{.33}$ photocathode was determined by comparison with a calibrated photocell using a sub-cathode diameter spot of 1060 nm light. As illustrated in Figure 6, the room-temperature quantum efficiency measured using this method was over 8% at 1060 nm. These values, however, turn out to be highly temperature dependent.

At a temperature of -20°C, the quantum efficiency rises to 9.7%. However, raising the temperature to 10°C lowered the quantum efficiency to 5.2%.

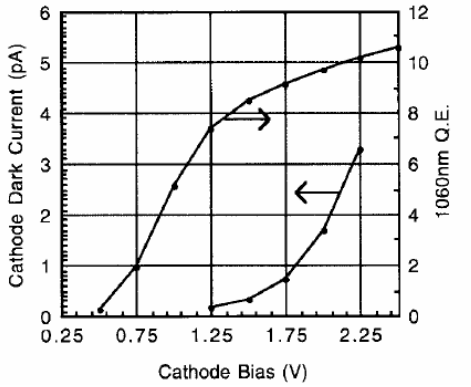

Figure 6: : Quantum efficiency of the $In_{.36}GA_{.31}As_{.67}P_{.33}$ photocathode

5.2 High Sensitivity GaAs Photocathode

Martin and Hink [11] report on a high sensitivity GaAs photocathode developed at Burle Industries. Utilizing the multichannel plate photomultiplier (MCPPMT) shown in Figure 7, photons pass through the faceplate of the PMT and initiate release of photoelectrons from the photocathode surface on the interior side of the faceplate. Due to a 300 V bias, the photoelectrons are accelerated toward the front surface of the first plate, colliding with the plate to create secondary electrons. This process continues down to the anode. Detection of red and infrared light has been reported with quantum efficiencies of greater than 20% using the MCPPMT scheme.

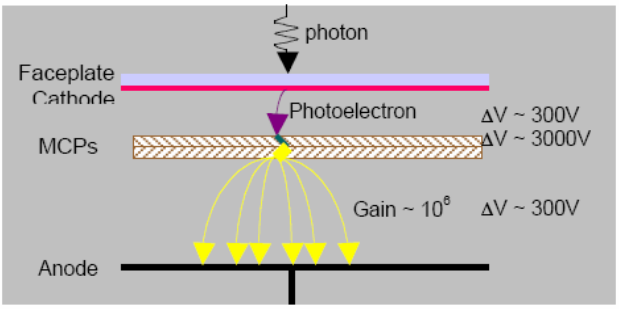

Figure 7: Schematic of GaAs multichannel plate PMT

6.0 References

[1] Hamamatsu Photonics. "Photomultiplier Tubes." http://sales.hamamatsu.com/assets/applications/ETD/pmt_handbook_complete.pdf.

[2] Burle Industries. "Photomultiplier Handbook." http://www.burle.com/cgi-bin/byteserver.pl/pdf/Photo.pdf.

[3] Image edited from Hamamatsu Photonics. "Photomultiplier Tubes." Figure 2-1. http://sales.hamamatsu.com/assets/applications/ETD/pmt_handbook_complete.pdf.

[4] Image edited from Hamamatsu Photonics. "Photomultiplier Tubes." Figure 2-2. http://sales.hamamatsu.com/assets/applications/ETD/pmt_handbook_complete.pdf.

[5] Bates, Clayton W. "Photoemission from Ag-O-Cs." Physical Review Letters. Vol 47(3), 20 July 1981, pp 204-208.

[6] Hallensleben, et al. "Limitations on the Enhancement of Photomultiplier Quantum Efficiency through Multiple Total Internal Reflection." J. Phys. D: Applied Physics 32(1999) pp 623-628.

[7] Image edited from Yariv, A., and P. Yeh. "Photonics: Optical Electronics in Modern Communications." 6th Ed. Figure 11.4, pp 504.

[8] Sommer, A. "The Element of Luck in Research – Photocathodes 1930 to 1980." J. Vac. Science Technology A, Vol 1(2), Apr 1983, pp 119-124.

[9] Morton, G. A. "Photon Counting." Applied Optics. Vol 7(1), Jan 1968, pp 1-10.

[10] La Rue, et al. "Photon Counting 1060-nm Hybride Photomultiplier with High Quantum Efficiency." IEEE Electron Device Letters, Vol. 20(3), Mar 1999, pp 126-128.

[11] Martin, J. and P. Hink. "Characterization of a Microchannel Plate Photomultiplier Tube with High Sensitivity GaAs Photocathode." 13th International Laser Ranging Workshop, 2002. http://cddis.nasa.gov/lw13/docs/papers/detect_martin_1m.pdf.

Matheson, R. "Recent Photomultiplier Developments at RCA." IEEE Transactions on Nuclear Science. Vol 11(3), June 1964, pp 64-71.

Saleh, B., and M. Teich. "Fundamentals of Photonics." pp 646-650.

Yariv, A., and P. Yeh. "Photonics: Optical Electronics in Modern Communications." 6th Ed. pp 501-511.